Journal of Catalysis **196,** 224–240 (2000)
doi:10.1006/jcat.2000.3045, available online at http://www.idealibrary.com on IDEAL®

Catalysis on Pd/WO_3 and Pd/WO_2

II. Effect of Redox Treatments in Hexanes and Hexenes Re-forming Reactions

C. Bigey[1] and G. Maire

*Laboratoire d'Etudes de la Réactivité Catalytique, des Surfaces et Interfaces, UMR 7515 du CNRS, ECPM, 25, rue Becquerel,
BP 08, 67087 Strasbourg, Cedex 2, France*

Received January 5, 2000; revised June 9, 2000; accepted August 24, 2000

Skeletal rearrangements of alkanes and alkenes were investigated on Pd/WO_3 and Pd/WO_2 catalysts following various activation treatments. Catalysts reduced at low temperature (350°C) are active and selective for isomerization of hydrocarbons. Palladium loses its intrinsic catalytic properties for isomerization but keeps partly its (de)hydrogenation properties. Hence we postulated that an interaction between palladium and tungsten oxide takes place under an H_2 stream. The catalysts exhibit high selectivity in isomerization which is linked to the presence of acidic active centers, mainly Brønsted sites, on WO_3 or $W_{20}O_{58}$ phases. Catalytic properties were interpreted by the traditional bifunctional mechanism, including the formation of carbocation species. Palladium metallic function, required for alkane dehydrogenation, deactivates with time under reactants but is easily regenerated by air exposure at 400°C. Striking results were obtained after exposures under oxygen and traces of water, providing an increase in the number of Brønsted acidic sites and in the acidity strength leading to an improvement of activity and isomerization selectivity. Catalysts reduced at higher temperature (600°C) are very active and selective for isomerization. Referring to our previous paper (35), devoted to catalyst characterizations (BET, TPR, XRD, XAS, XPS), we suggested that catalytic properties are then due to the W_3O phase. The catalytic behaviour of such a phase has been interpreted with a monofunctional mechanism including tungstenacyclobutane species as intermediates. © 2000 Academic Press

Key Words: **Pd/WO_3, Pd/WO_2 catalysts; hydrocarbons cracking, isomerization; surface states, mechanisms, acidity.**

I. INTRODUCTION

The catalytic properties of tungsten oxides have been widely studied for olefin metathesis (1–4) but also for other applications, mainly oxidation of propene (5) and isomerization of butenes (6–9). Some studies have suggested the potential application of bulk tungsten oxides for re-forming reaction (10–13). Although the results seemed to be attractive, they pointed out the difficulty in obtaining stable catalytic properties and, consequently, in correlating catalytic properties with surface states (10). Moreover, fresh bulk WO_3 is inactive toward saturated hydrocarbons as shown by Katrib *et al.* for 2-methyl-pentane (11–13). On the other hand, palladium is well known for its hydro–dehydrogenation character (14) and its skeletal rearrangement properties (15–20). The goal of this research was to obtain active, selective, and stable catalysts for the skeletal rearrangement of hydrocarbons. So, our strategy was to add the palladium to tungsten oxides. Some studies have shown that an interaction of the metallic phase with a support could induce great modifications of the catalytic properties, especially in the case of reducible supports (21–24). To our knowledge, catalysts constituted by palladium supported on bulk tungsten oxides have never been mentioned in the literature as re-forming catalysts but they were mentioned for other applications: selective hydrogenation (25), automotive exhaust treatment (26), and carbon monoxide hydrogenation (27). However, some other works have been devoted to study the re-forming properties of catalysts constituted by a metal (Pt or Pd) added to tungsten oxides deposited on Al_2O_3 (28–30), SiO_2 (31, 32), and more recently ZrO_2 (33, 34) supports. These studies pointed out the great importance of preparation methods, especially the metal and tungsten oxide loading, on the selectivity toward isomerization or hydrogenolysis. Regardless of these observations and to achieve our objectives, we have focused our attention on the procedure to prepare palladium-based catalysts using WO_2 and WO_3 as supports and on the conditioning of such catalysts (reduction temperature, oxidation). The results presented in Part I of this series (35) were devoted to surface state characterizations as a function of various treatments employed for the catalytic tests presented here in Part II. Correlations between the catalytic data and the surface states of the samples have been established.

---

[1] To whom correspondence should be addressed. Fax: 33 03 88 13 69 61. E-mail: maire@chimie.u-strasbg.fr.

0021-9517/00 $35.00

2. EXPERIMENTAL

2.1. Catalyst Preparations

The supported catalysts were prepared by "wet" impregnation of the tungsten oxide supports with an aqueous solution of tetrammine palladium(II) chloride in order to obtain 1 wt% Pd in the final sample. $Pd(NH_3)_4Cl_2 \cdot H_2O$ was provided by Johnson & Matthey. WO_3 and WO_2 supports were supplied by Strem Chemicals. The initial specific surface areas are 1.5 m^2/g and 0.15 m^2/g, respectively. Previous studies by XPS have reported that the surface of WO_2 was contaminated by some WO_3 layers after exposure under air. With regard to this observation, the WO_2 support was submitted to a prereduction to obtain, as much as possible, a clean WO_2 surface before impregnation with the Pd salt. The same treatment was applied to prepare a Pd/WO_3 catalyst for comparison. The catalysts were identified as Pd/(WO_3calc), Pd/(WO_3red), and Pd/(WO_2red).

Pd/(WO_3calc). Bulk WO_3 was submitted to a treatment in air flow at 400°C for 15 h. After cooling to room temperature, the support was impregnated with the solution of palladium salt. The excess solvent was evaporated and the catalyst calcined under an air flow at 400°C for 4 h after drying. A heating rate of 10°C min^{-1} was used.

Pd/(WO_3red). Prior to Pd deposition, bulk WO_3 was reduced in hydrogen at 350°C for 15 h. After cooling to room temperature, the catalyst was kept under an argon flow to prevent any reoxidation. The WO_3 support was then impregnated rapidly and the catalyst was dried in air at 110°C overnight. It was used for catalytic tests without any calcination step.

Pd/(WO_2red). The catalyst was prepared as Pd/(WO_3red) using WO_2 as support. Pd/Al_2O_3 catalyst, used as palladium reference, was obtained after γ-Al_2O_3 (RP, GC064, 206 m^2/g) impregnation with the solution of palladium salt and dried in air at 110°C. WO_3 and WO_2 bulk oxides were used without any treatment. Table 1 summarizes the catalysts, metal, and chlorine contents and pretreatments.

2.2. Apparatus and Procedures

Reactants. The main hydrocarbons used in catalytic tests were 2-methyl-pentane (2MP) and 4-methyl-1-pentene (4M1Pn), supplied by Fluka (puriss > 99.5%). Hydrogen was used after purification by a gas-cleaning filter system (Chrompack) in order to remove trace amounts of oxygen and moisture.

Catalytic experiments. The experiments were performed in a plug flow reactor at atmospheric pressure (29). The gas flows were fixed by using a mass flow controller. The reactants were introduced via a septum in a saturator which was immersed in a cooling bath, the temperature of which was set at −37.5°C. The following partial pressure (Torr) ratios were $P_{(2MP)}/P_{H_2} = 6.6/753.6$ and $P_{(4M1Pn)}/P_{H_2} = 9.7/750.3$. A double thermal conductivity detector system (TCD) controls the contact time of reactants and products. The typical quantity of hydrocarbons injected for a catalytic test was 5 μl (pulse) which in the case of the 2MP and 4M1Pn reactants corresponds to a steady-state feed above 6 and 4 min, respectively. After 2 min, the products were sampled and analyzed on-line by gas chromatography using a 50-m (CP-SIL-5CB) column and a flame ionization detector. A Pt catalyst at 110°C placed before the CPG allows in some cases hydrogenation of the olefins which could be produced during the catalytic experiments and complicate the analysis. In the present study, the gas flow used for treatments and catalytic tests was fixed at 30 cm^3 min^{-1}, and the reaction temperature was 350°C. The mass of catalysts used was 100 mg for samples containing tungsten oxide and 50 mg for the Pd/Al_2O_3 reference to keep the conversion below 30% and avoid secondary reactions.

Catalytic tests procedures. The catalysts were reduced *in situ* under a hydrogen flow at 350°C (LTR) or 600°C (HTR). The catalytic properties were studied as a function of exposure time under H_2 at 350°C or 600°C except in the case of the Pd/Al_2O_3 catalyst which was tested after 15 h of reduction at 350°C or 600°C.

—"LTR" treatment denotes a reduction at low temperature. The temperature was raised from room temperature

TABLE 1

Weight Percentages of Metal and Chlorine, and Methods of Pretreatments for the Supports and Catalysts

Catalysts	BET[a] supports (m^2/g)	Pretreatments of the supports	Pd[b] (wt%)	Cl[b] (wt%)	Pretreatment of the catalysts (*ex situ*)	BET catalysts (m^2/g)
Pd/Al_2O_3	206	Dried at 110°C overnight	0.89	0.84	Calcined at 350°C, 2 h	205
Pd/(WO_3calc)	1.5	Calcined at 400°C, 15 h	0.87	560 ppm	Calcined at 400°C, 4 h	7
Pd/(WO_3red)	1.5	Reduced at 350°C, 15 h	0.93	0.65	Dried at 110°C overnight	5
Pd/(WO_2red)	0.5	Reduced at 350°C, 15 h	0.93	0.48	Dried at 110°C overnight	1

[a] Initial specific surface areas of supports.

[b] Chemical analysis obtained by atomic absorption (CNRS-Lyon).

to 350°C by using a ramp of 10°C min^{-1}. The time under H_2 was taken into account once the temperature of 350°C was reached. The temperature was maintained throughout all catalytic tests. This temperature was chosen in reference to results obtained in our laboratory on bulk WO_3 samples reduced under H_2 at 330°C leading to steady-state conditions.

—"O400" denotes an oxidation under air at 400°C for 1 h. First, catalysts were submitted to LTR treatment. As soon as the catalysts showed stable properties, the oxidation treatment was applied. The procedure was to decrease the temperature from 350°C to 25°C (under H_2), purge the reactor under N_2, and switch under air for 15 min. The temperature was then raised from 25°C to 400°C (heating ramp 10°C min^{-1}). The reactor was maintained at 400°C for 1 h and the temperature was decreased to room temperature. The system was again purged under N_2 and then the standard LTR treatment was used.

—Oxidation treatment under a $[H_2O + O_2 + N_2]$ mixture at 350°C. The aim of such treatment was to show the influence of controlled amounts of water on catalytic performances. It was performed under a controlled $[O_2 + H_2O + N_2]$ mixture containing 225 ppm H_2O and 80 ppm O_2 in N_2 (calibrated by mass spectrometry). The catalysts were submitted to LTR treatment over a limited period (6 h) while catalytic properties were studied by using 2MP and 4M1Pn hydrocarbons (named series a). Hydrogen was then replaced by the $[N_2 + O_2 + H_2O]$ mixture for 12–15 h. A new LTR treatment was carried out for 8 h with catalytic tests (named series b). In the same way, two other series of experiments were carried out (series c and d).

—"HTR" treatment denotes a reduction at high temperature (600°C). The temperature was initially raised from room temperature to 600°C (10°C min^{-1}). The temperature was chosen well above 420°C to produce the largest modifications of tungsten oxide properties as already observed by Cornet and Travert (37). After 30 min at 600°C, the temperature was decreased to 350°C and the catalytic properties were studied with the 2MP and 4M1Pn. The temperature was then quickly raised back to 600°C to minimize the time under H_2 between 350°C and 600°C which was not taken into account.

Catalytic data. The conversion (αt) is defined as the percentage of reactant transformed (number of moles converted over the number of moles introduced × 100). The reaction rate is given as the number of moles converted per gram of catalyst per second ($\text{mol} \cdot \text{g}^{-1} \text{s}^{-1}$). This rate is calculated by assuming a first-order reaction and is given by $r = (F/w) \ln(1/(1 - \alpha t))$, with $F =$ molar flow rate ($\mu\text{mol} \cdot \text{s}^{-1}$) and $w =$ weight of catalyst (g). The selectivity of a product is expressed as the percentage of this product among all the products obtained. S_{iso} is the selectivity in isomers. Starting from 2MP or 4M1Pn, the 3MP/HEX ratio is representative of the catalyst acidity (36).

3. REACTIVITY OF HYDROCARBONS

3.1. Catalysts Reduced Following the LTR Procedure

The catalytic properties (activity, selectivity) change progressively under the H_2 flow and the reactant mixture at 350°C untill a stable state is reached. For the sake of clearness, we will analyze first the catalytic results after a short period (0.25 h) under H_2 at 350°C, and then the influence of time of exposure to hydrogen stream, and last we will examine the aging under a continuous 4M1Pn/H_2 mixture.

3.1.1. Catalytic data during the initial exposure to H_2 at 350°C. Pd–W-based catalysts were submitted to H_2 treatment following the LTR procedure. After 0.25 h of exposure to H_2 at 350°C, the first catalytic test is performed by introduction of the 2MP (5 μl) and after that the 4M1P (5 μl) was tested. The data are collected in Table 2 with those gained on bulk WO_3 and WO_2 powders and a classical Pd/Al_2O_3 catalyst. Pd/(WO_3calc), Pd/(WO_3red), and Pd/(WO_2red) are active for skeletal rearrangement of both 2MP and 4M1Pn hydrocarbons. The reaction rate is higher for the olefin compared to the paraffin. In the same conditions, bulk WO_3 and WO_2 are inactive toward the saturated hydrocarbon. The selectivity in isomerization is very interesting when compared to those obtained with the Pd/Al_2O_3 reference and approaches those of bulk WO_2 samples (case of 4M1Pn). 3MP is formed in large amounts. The 3MP/HEX ratio indicates some differences in the acidity character of the catalysts. The ratio is high, in the range 11–8, for Pd/(WO_2red) and lower, in the range 1–4, for Pd/(WO_3calc) and Pd/(WO_3red). The reactions of cracking are low and propane is the major product. Some traces of MCP are detected (around 2–3%). At this stage, the palladium allows dehydrogenation and hydrogenation reactions, as expected. But as deduced from the distribution products palladium seems to play a minor part in the skeletal rearrangement of hydrocarbons (no selective demethylation and very low isomerization via cyclic mechanism). Tungsten oxides favor the isomerization reactions as already observed (38). These data suggest as expected that Pd–W-based catalysts develop bifunctional properties.

3.1.2. Influence of time exposure to H_2 at 350°C. The influence of time of exposure to H_2 was investigated by using 2MP and 4M1Pn. The catalytic tests were always performed by introduction of a 5-μl pulse of reactant. 2MP and 4M1Pn were tested on the same catalytic sample for Pd/(WO_3calc) and Pd/(WO_3red) and on separate samples for Pd/(WO_2red) catalyst. Between two pulses, the catalytic bed was maintained under H_2 at 350°C. In Fig. 1 are collected the conversion, the selectivity in isomers, and the 3MP/HEX ratio. Tungsten-based catalysts lose their activities for the 2MP hydrocarbon, especially in the case of Pd/(WO_3calc) and Pd/(WO_3red) which show a short-lived catalytic activity. Pd/(WO_2red) catalyst remains

TABLE 2

Product Distribution of 2MP and 4M1Pn on Pd/(WO$_3$calc), Pd/(WO$_3$red), and Pd/(WO$_2$red) after 15 min of H$_2$ Exposure at 350°C: Comparison with WO$_3$, WO$_2$, and Pd/Al$_2$O$_3$ Samples

Catalysts	HC	t (h)	$\alpha(t)$ (%)	r (μmol/g·s)	Siso (%)	3MP/HEX	C1	C2	C3	C4	C5	22DB	23DB	3MP	HEX	MCP
Pd/(WO$_3$calc)	2MP	0.25	43.1	0.65	81.1	1.4	2.2	1.8	11	1.6	1.2	8.4	9.9	37.1	25.8	Traces
	4M1Pn	0.25	50.4	1.31	51.2	1.0	Traces	1.6	33.6	4.8	4.2	2.4	5.4	21.8	21.6	Traces
Pd/(WO$_3$red)	2MP	0.25	27.6	0.34	92.5	4.1	1.5	1.3	1.3	0.8	0.6	3.7	8.6	64.6	15.6	1.8
	4M1Pn	0.25	51.3	1.10	93.3	2.7	1.6	0.9	2.3	0.7	0.6	5.4	10.8	56.3	20.8	0.7
Pd/(WO$_2$red)	2MP	0.25	18.3	0.25	74.6	10.5	8.3	3.8	2.2	2.6	2.6	0.6	5.2	62.7	6.0	5.8
	4M1Pn	0.25	28.3	0.60	91.2	7.9	3.1	1.8	1.7	1.1	1.0	1.2	6.0	72.6	9.2	2.1
WO$_3$	2MP	0.25	0	—	—	—	—	—	—	—	—	—	—	—	—	—
	4M1Pn	0.25	57.4	0.98	90.5	2.2	Traces	Traces	3.1	3.1	2.3	Traces	16.7	53.8	19.1	0
WO$_2$	2MP	4	0	—	—	—	—	—	—	—	—	—	—	—	—	—
	4M1Pn	4	4.1	0.12	99.4	27.0	0	0	Traces	0	0	0	2.3	93.3	3.5	0
Pd/Al$_2$O$_3$	2MP	15	26.1	0.98	10.8	1.2	41.1	0.6	1.0	2.9	35.8[a]	0	Traces	5.8	5.0	7.3
	4M1Pn	15	18.5	1.17	9.7	1.3	41.2	0.6	1.0	2.4	34.7[a]	0	Traces	5.4	4.3	9.6

[a] C5 = isopentane + pentane + cyclopentane.

active longer for 2MP ($\alpha_{(1\,h)} = 17\%$, $\alpha_{(70\,h)} = 8\%$). However, the catalysts maintain their activities toward 4M1Pn. These observations suggest a deactivation of hydro–dehydrogenation sites. This is confirmed by the olefin percentages in the products obtained with 4M1Pn, 43% with Pd/(WO$_3$calc) and 75% with Pd/(WO$_3$red) after 7 h under H$_2$ at 350°C. Whatever the catalyst, no signs of reversible deactivation for 2MP are observed under H$_2$ even after exposure up to 12–15 h without catalytic tests (Fig. 1a). The metallic function, supposed to be due to Pd, is deactivated during H$_2$ exposures (modification of the surface states) or/and after carbonaceous residues deposition. 4M1Pn reactivity is affected during catalytic "runs" (i.e., successive catalytic tests) but improved after long exposure under H$_2$ without test. This phenomenon is obvious for Pd/(WO$_2$red) catalyst which shows an abrupt increase of the conversion after H$_2$ exposures. The overall selectivity in isomerized products obtained for the 4M1Pn reactant increases as a function of time under H$_2$ and catalytic tests and reaches a maximum of 83% for Pd–WO$_3$-based catalysts and 85–97% for Pd/(WO$_2$red) catalyst (Fig. 1b). A great decrease in the selectivity is obtained after long time exposure under H$_2$ (without hydrocarbon) except in the case of 2MP for the Pd/(WO$_2$red), for which S$_{\text{iso}}$ remains almost unchanged and exhibits a stable global selectivity. After the first stage under catalytic tests, the 3MP/HEX ratio is stable to 1.5–2 values for Pd–WO$_3$-based catalysts and seems unaffected by exposure to H$_2$ (Fig. 1c). At this stage, the Pd/(WO$_3$red) and Pd/(WO$_3$calc) samples exhibit identical properties. Pd/(WO$_2$red) sample has a peculiar behavior, leading to a slower decrease of the ratio and keeping interesting values. The decrease occurs faster for 4M1Pn than for 2MP. No modifications of tendencies are induced by pure H$_2$ exposures. In fact, this latter observation is different from the observations when the reactivities of 2MP and 4M1Pn were studied alternatively on the same catalytic sample. Indeed, the decrease of the 3MP/HEX ratio was faster for 2MP. This trend demonstrates the influence of 4M1Pn reactant on the catalytic performances. Comparing the 3MP/HEX ratios for Pd/WO$_x$ catalysts, it appears that the acidic character is initially stronger for Pd/(WO$_2$red) and remains longer. This phenomenon is probably due to surface state evolutions which are not identical for all catalysts. The changes in isomer distributions are reported in Fig. 2 for Pd/(WO$_2$red). The results show that the decrease in 3MP/HEX ratio is due to an increase in HEX and to a decrease in 3MP formation. 23DB is formed in a significant amount. Only traces of 22DB are detected. Small amounts of MCP are initially formed. We noted that the disappearance of MCP in the product distributions is always accompanied by a decrease of C1 in favor of C3. The distribution of cracked products show very low modifications, giving mainly C3.

3.1.3. Aging effects under stream of reactants (4M1Pn/H$_2$). Catalysts were pretreated under H$_2$ at 350°C for 1 h. A 100-μl portion of reactant was injected corresponding to a time of 90 min under the reaction mixture under our operating conditions. A change in activity was studied as a function of time under the 4M1P/H$_2$ stream. In all cases, as mentioned above, Pd/WO$_x$ activities toward 4M1Pn are very high. The conversion remains unchanged versus time on stream. The selectivity in isomers for Pd/(WO$_3$calc) and Pd/(WO$_3$red) increases from 65% to 90% during the first 30 min. This phenomenon is weaker for Pd/(WO$_2$red) catalyst, which is initially very selective for isomerization

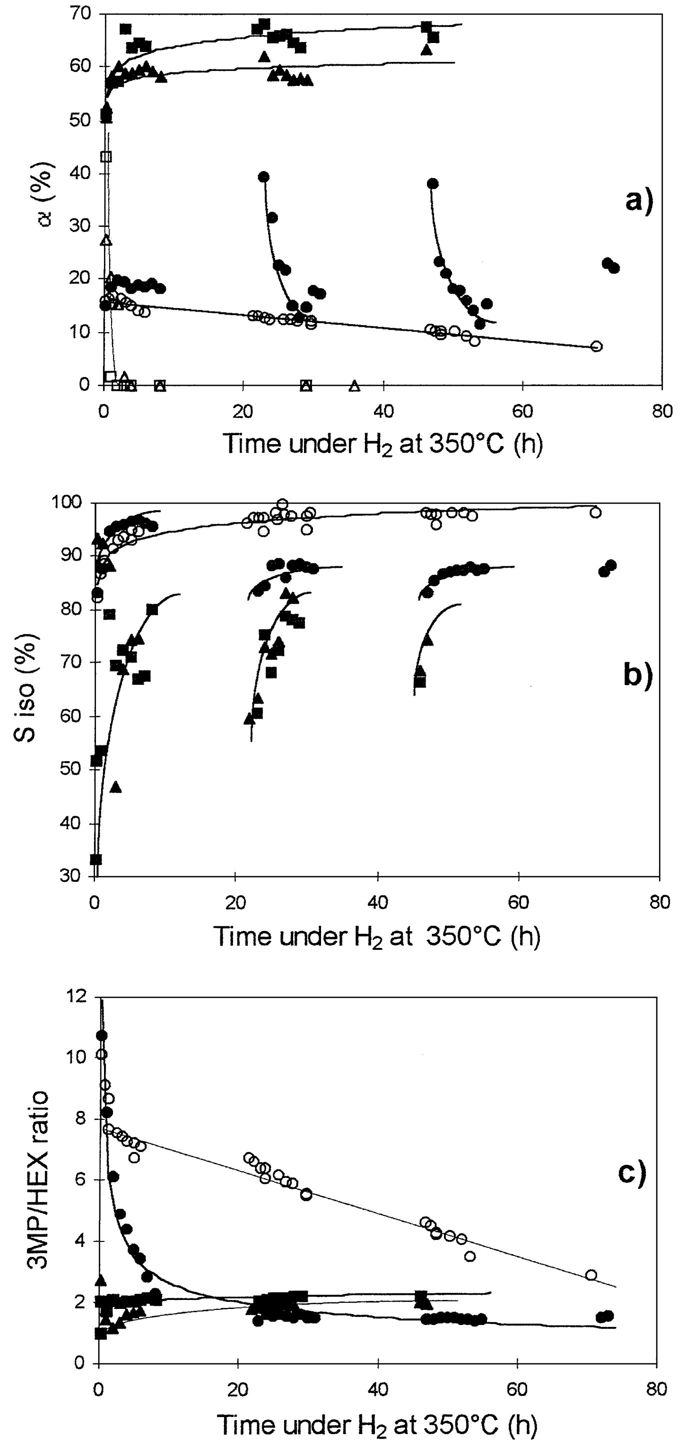

FIG. 1. Evolution of catalytic properties versus time under H_2 at 350°C on Pd/(WO_3calc)–2MP (☐), 4M1Pn (■), Pd/(WO_3red)–2MP (△), 4M1Pn (▲), and Pd/(WO_2red)–2MP (○), and 4M1Pn (●). Conversion (a), selectivity in isomers (b), and 3MP/HEX ratio (c).

starting from 90% up to a maximum of 97%. These evolutions are illustrated in Fig. 3, in the case of Pd/(WO_3calc), showing the distribution of cracked and isomerized products. Similar results are obtained for the two other catalysts. The increase in isomerization selectivity in favor of 3MP is mainly due to a faster decrease of propane. These features confirm that no deactivation of catalysts toward 4M1Pn occurs under continuous 4M1Pn/H_2 mixture. Only small changes in product distributions are initially observed due to some deactivation of sites responsible for acidic cracking processes.

3.2. Influence of Oxidative Treatments

3.2.1. Influence of an oxidative treatment under air at 400°C. Catalysts were studied following the LTR treatment. As soon as the catalytic properties were stable, the catalysts were submitted to an oxidation treatment following the O400 procedure. After that a new reduction treatment was applied. The main catalytic results obtained with the 2MP are presented in Fig. 4. The oxidation treatment induces two phenomena for Pd–WO_3-based catalysts. The first is to restore and the second to improve activity. The 2MP conversion, initially above 40 and 30%, reaches after oxidation 45 and 50% for Pd/(WO_3calc) and (Pd/WO_3red), respectively. However, the oxidation treatment is not sufficient to the maintain activity of the catalysts toward 2MP and the conversion decreases rapidly to zero. The product distribution is not modified except for a slight increase in C1 and MCP products which further decrease versus time under H_2. Oxidation does not induce specific changes in the overall selectivity in isomers and in the 3MP/HEX ratio. The oxidation treatment on Pd/(WO_2red) catalyst is peculiar. It restores the initial conversion and selectivity in isomers obtained on fresh samples but especially leads to a spectacular increase in the 3MP/HEX ratio which could be associated with an increase in the acidity strength. The ratio is then close to the value obtained on bulk WO_2 (Table 2).

The effect of similar oxidative treatment was examined for Pd–WO_3-based catalysts for the 2MP reactant. The only difference from the previous treatment is that the 2MP reactivity was tested only after 15 h of exposure to H_2 (before and after the oxidation). An interesting result was the observation of a catalytic activity toward 2MP with a conversion which turned around 5% and 20% before and after the oxidation, respectively, while the conversion was zero for the same time of H_2 exposure with catalytic tests. With regard to these observations, it appears that the metallic function, very sensitive to hydrocarbon adsorption, is developed after an oxidative–reductive treatment.

3.2.2. Influence of treatments under [$N_2 + O_2 + H_2O$] mixture at 350°C. The influence of traces of water was examined for the Pd/(WO_2red) sample with a [$N_2 + O_2 + H_2O$] mixture at 350°C. The results are collected in Figs. 5 and 6. The first series of experiments (series a) shows a decrease in 2MP activity which occurs quicker by comparison to what was observed when 2MP and 4M1Pn were tested on separate samples (Section 3.1.2). This confirms

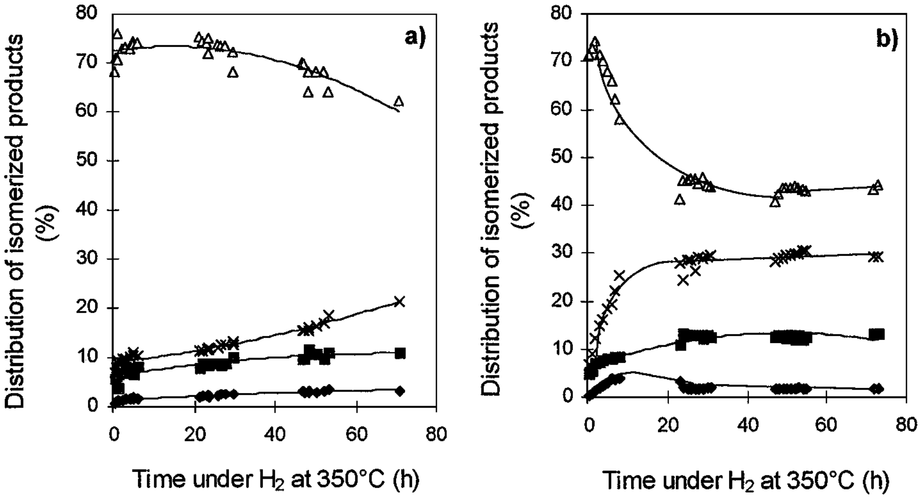

FIG. 2. Distribution of isomerized products: 22DB (◆), 23DB (■), 3MP (△), and HEX (×) on $Pd/(WO_2red)$ catalyst versus time under H_2 at 350°C for (a) 2MP and (b) 4M1Pn.

that 4M1Pn reactant accelerates the deactivation of metallic sites. After exposure to a $[O_2 + H_2O + N_2]$ mixture, the 2MP conversion restarts at high values and then decreases again with the repeated catalytic tests. S_{iso} increases during catalytic tests from 80% to 95% (series a) but becomes increasingly smaller after each exposure to oxidizing mixture (88%). The 3MP/HEX ratio illustrates very well the modification in acidity strength due to $[O_2 + H_2O + N_2]$ exposure. Indeed, the 3MP/HEX ratio value starts at 10 at the beginning of series a and reaches 18 at the beginning of series d. During a series, the cracked products decrease (C1 being always the major product) in favor of isomerized products, showing an interesting selectivity in 3MP isomer (Fig. 6). This signifies a progressive poisoning of the cracking sites, mainly metallic sites. After each $[O_2 + H_2O + N_2]$ exposure, the cracking reaction is promoted with the methane reappearance, accompanied by the formation of some MCP (~5%). HEX formation is hindered and becomes smaller and smaller in favor of 3MP. The influence of treatments under the $[O_2 + H_2O + N_2]$ mixture results in an increase in the acidity strength and the regeneration of the metallic sites.

3.3. *Catalysts Reduced Following the HTR Procedure*

Reduction at 600°C induces drastic changes in the behavior and generates very active catalysts for both 2MP and 4M1Pn reactants. An induction period under H_2 is

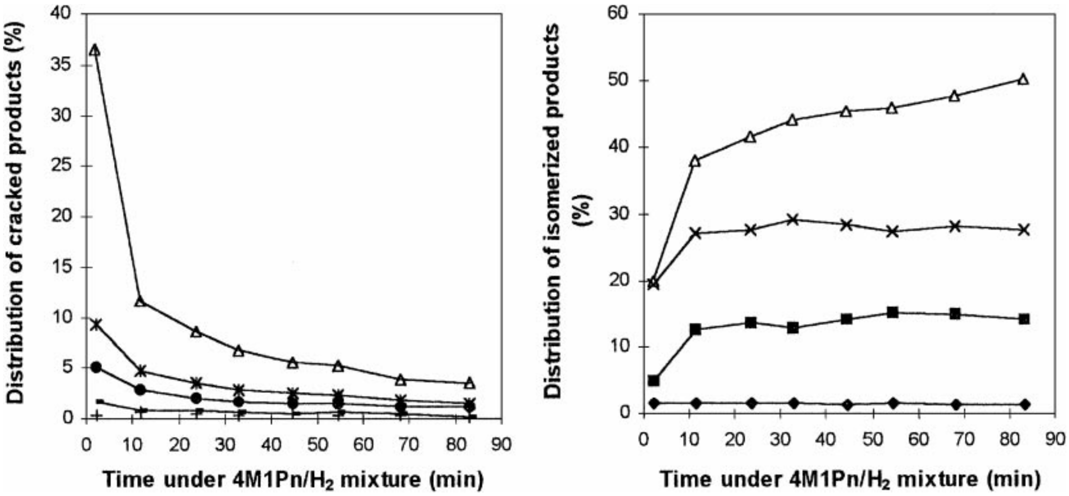

FIG. 3. Aging effects under reactants stream (4M1Pn/H_2) on $Pd/(WO_3calc)$ catalyst reduced at 350°C for 1 h. Distribution of cracked products: C1 (+), C2 (−), C3 (△), C4 (∗), and C5 (●). Distribution of isomerized products: 22DB (◆), 23DB (■), 3MP (△), and HEX (×).

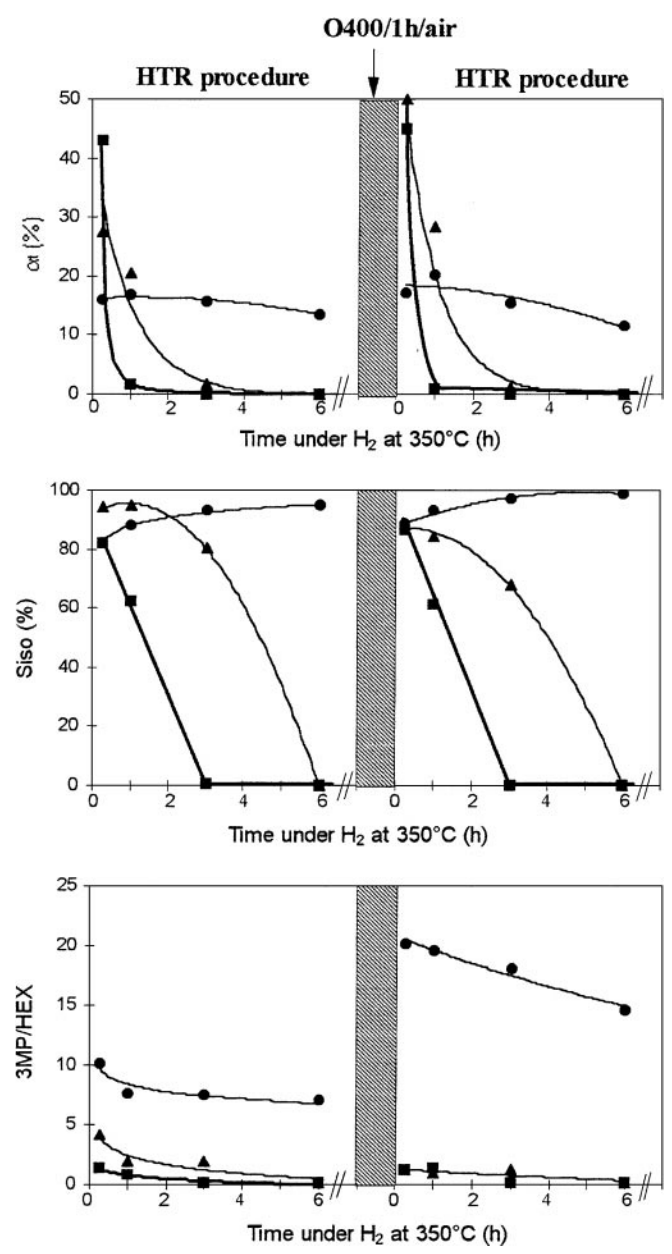

FIG. 4. Influence of oxidative treatment under air at 400°C for 2MP reactivity on Pd/(WO_3calc) (■), Pd/(WO_3red) (▲), and Pd/(WO_2red) (●) catalysts.

necessary to obtain stable properties (Table 3). During this period, the overall selectivity in isomers for the Pd–WO_3-based catalysts increases to reach interesting values (75–90%). Pd/(WO_2red) catalyst gives values around 85%. The isomerized products decrease in the following order: 3MP > HEX > 23DB, 22DB. A study as a function of catalyst weight led us to conclude that 22DB was formed by secondary reactions. The 3MP/HEX ratio is close to 3.5 which is representative of an acidic character. The distribution of cracked products clearly shows that selective demethylation (C1 + C5) and β-scission are the major reactions during the first stage of reduction (1 h) whereas demethylation is mainly obtained under stable conditions (15–20 h). Among all the products, MCP is present in low amounts. The different kinds of Pd/WO_x catalysts show similar activities. The difference between the reactivities of 2MP and 4M1Pn, initially observed, becomes smaller as a function of time under

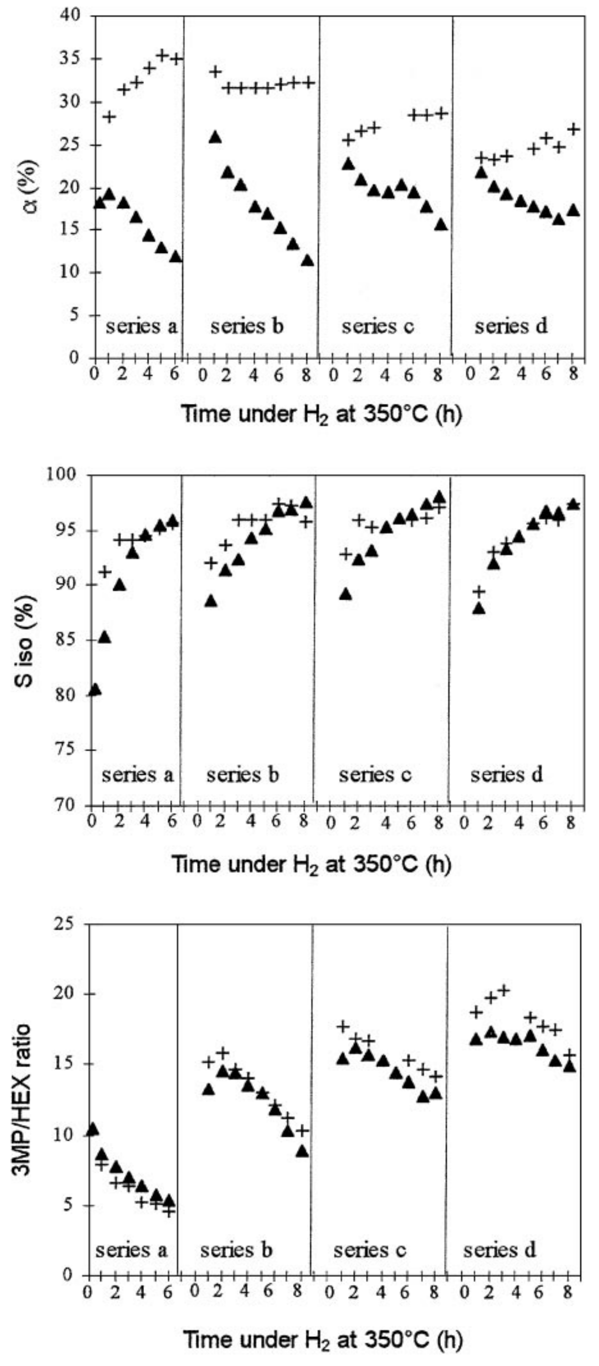

FIG. 5. Influence of oxidative treatment under the [$O_2 + H_2O + N_2$] mixture at 350°C on Pd/(WO_2red) catalytic properties for 2MP (▲) and 4M1Pn (+). The vertical lines symbolize the time of exposure under the mixture (12–15 h).

TABLE 3

2MP and 4M1Pn Reaction on Pd/(WO_3calc), (Pd/WO_3red), Pd/(WO_2red), and Pd/Al_2O_3 Catalysts Reduced at 600°C: Comparison with Bulk WO_3 and WO_2

Catalysts	HC	t (h)	$\alpha(t)$ (%)	r (μmol/g · s)	Siso (%)	3MP/HEX	C1	C2	C3	C4	C5	22DB	23DB	3MP	HEX	MCP
Pd/(WO_3calc)	2MP	1	65.3	0.79	64.9	1.5	11.5	2.2	7.3	33.1	8.1	9.3	7.6	28.8	19.2	0.6
	2MP	15	52.6	0.70	71.9	3.9	11.5	2.5	3.2	2.5	8.4	5.3	5.8	46.4	12.0	2.3
	4M1Pn	1	61.0	1.16	76.5	2.2	6.6	1.6	5.6	2.5	5.1	11.0	9.0	38.7	17.8	0.7
	4M1Pn	15	52.1	1.01	85.0	3.7	5.4	1.1	1.7	1.6	3.7	5.7	7.4	55.7	16.4	2.0
Pd/(WO_3red)	2MP	1	44.5	0.98	66.1	1.3	4.5	1.9	19.3	5.6	5.7	9.7	6.7	19.2	16.8	ε
	2MP	20	50.5	1.14	85.1	3.7	5.0	1.1	2.2	1.2	3.6	6.3	5.9	57.4	15.5	1.7
	4M1Pn	1	49.4	0.83	59.0	1.3	1.4	1.9	29.8	4.5	3.0	3.5	7.7	26.6	21.1	ε
	4M1Pn	20	51.7	1.21	90.0	3.2	2.6	0.7	2.0	1.0	2.2	7.3	7.0	57.8	18.0	1.4
Pd/(WO_2red)	2MP	1	32.2	0.48	85.1	6.8	5.0	1	1.5	1.1	3.3	1.7	5.6	67.8	10.0	2.7
	2MP	20	47.6	0.80	81.3	3.8	6.5	1.3	2.1	1.5	5.2	3.6	5.7	56.6	15.1	2.1
	4M1Pn	1	43.9	0.92	90.4	3.5	3.2	0.7	1.2	0.9	2.1	0.94	6.9	70.8	10.6	1.4
	4M1Pn	20	47.6	1.04	85.0	3.9	4.8	1.1	1.9	1.3	3.9	3.6	5.5	60.3	15.5	1.8
Pd/Al_2O_3	2MP	15	5.6	0.15	26.9	1.6	11.6	0.8	1.0	1.1	15.4[d]	0	0.8	16.1	10.0	41.5
	4M1Pn	15	4.1	0.14	26.7	2.0	11.0	0.8	1.6	0.9	11.5[d]	0	Traces	17.8	8.7	47.2
WO_3[a,b]	2MP	1	51.1	—	73.4	1.3	10.8	4.9	10.4	6.2	6.4	4.7	8.7	26.0	21.7	0
WO_3[a,c]	2MP	5	41.7	—	85.2	3.0	4.2	1.9	2.8	2.3	3.6	2.6	8.1	56.0	18.4	0

[a] Results obtained in our laboratory (F. Hemming, Thesis, 1996).

[b] Weight of catalyst, 200 mg; hydrogen flow, 54 cm^3 min^{-1}; reduction at 520°C for 1 h (without heating ramp from room temperature to temperature of reduction).

[c] Weight of catalyst, 200 mg; hydrogen flow, 54 cm^3 min^{-1}, reduction at 420°C for 5 h.

[d] C_5 = isopentane + neopentane + cyclopentane.

H_2 which suggests that the reaction mechanism is modified. As pointed out previously for tungsten-based catalysts reduced at 350°C the properties are different from those of classical Pd/Al_2O_3 catalysts treated in similar conditions. The present results obtained on Pd–W-based catalysts show similarities to those obtained in our laboratory on bulk powder WO_3 reduced at 520°C for 1 h; in fact, the best agreement is obtained with bulk WO_3 reduced at 420°C for 5 h. It is important to mention that whatever the time of exposure to H_2, the catalysts remain selective for isomerization and no deactivation toward 2MP has been noticed. At this stage, we are not certain that the metallic character belongs exclusively to palladium. Results obtained with HEX, MCP, and 22DB hydrocarbons (not presented in this article) confirm

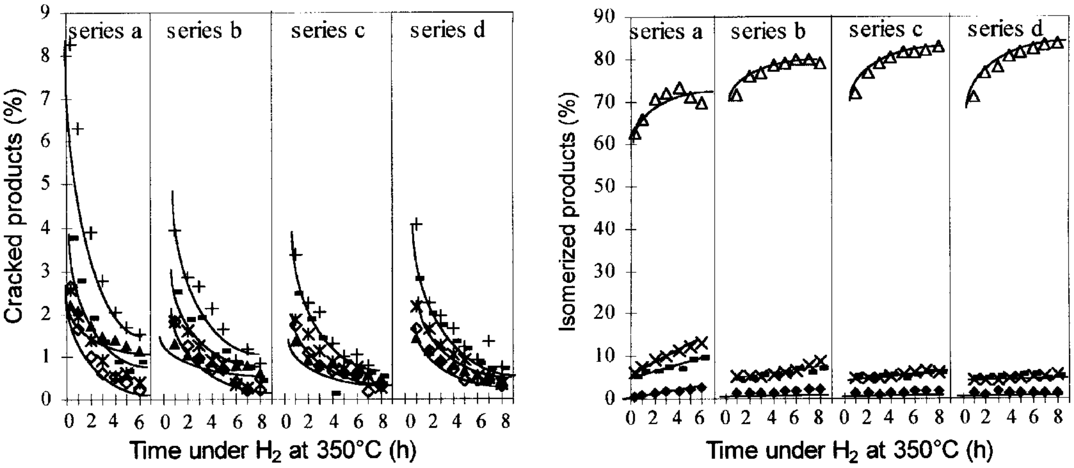

FIG. 6. Evolution of product distributions versus [$O_2 + H_2O + N_2$] exposures at 350°C obtained on Pd/(WO_2red) catalyst for 2MP. Distribution of cracked products: C1 (+), C2 (−), C3 (▲), C4 (✖), and C5 (◇). Distribution of isomerized products: 22DB (◆), 23DB (−), 3MP (△), and HEX (×).

the results obtained with 2MP. Indeed, HEX gives 2MP and 3MP predominantly, MCP leads to cyclohexane, and 22DB is isomerized in 23DB.

4. GENERAL DISCUSSION

4.1. Catalytic Properties in Correlation with Surface States—Role of Palladium

Catalysts submitted to LTR treatments. Adding a metal function (1 wt% Pd) to WO_2 or WO_3 leads to catalysts active toward saturated hydrocarbons after a short induction time under H_2 at 350°C whereas for the same treatment (under our operating conditions), bulk oxides remain inactive. It has been reported that an induction time under H_2 was necessary to obtain an activity from WO_3 toward alkane isomerization (9, 11, 13). Indeed, the activity was attributed to bulk structural rearrangements resulting in WO_{3-x} phases. The same observation was obtained for WO_2 resulting from a contamination of the surface by WO_3 (11, 12, 35, 39). On the other hand, it is known that the water vapor produced during reduction is a limiting factor of the kinetic reduction of bulk WO_3 as mentioned in our previous paper (35) and by several authors (40–42). However, a lot of parameters, such as the weight of sample, height of catalytic bed, flow, etc., are important and influence the reduction process and consequently, the catalytic properties. Otherwise our results show a positive contribution of Pd to the catalytic activity when associating Pd and W oxides. We have shown by the TPR technique that Pd influences also the reduction process of tungsten oxides and has a promoting effect on the reduction of these supports (35). By means of thermogravimetric analysis, Sancier investigated the effect of palladium on the rate of reduction by H_2 on WO_3 (43). The results suggested that the presence of metal decreases the reduction temperature of the oxide, presumably by dissociation of molecular hydrogen followed by migration of H atom on the support. These results were in agreement with other studies on WO_3 in the presence of Pt–Al_2O_3 (44) and on a mixture of WO_3 with platinum (45). Platinum was also found to catalyze the reduction of tungsten oxide species for Pt/WO_x–ZrO_2 systems (46, 47). The difference in activity between catalysts (Pd(WO_3calc) > Pd(WO_3red) > Pd(WO_2red)) results probably from the dispersion of palladium largely depending on the initial specific areas of the supports (1.5 and 0.15 m^2/g for WO_3 and WO_2) and on the pretreatment of supports (reduction or calcination). Such an explanation is suitable from the Pd/W atomic ratios deduced by XPS results (35), which can provide an indication of the dispersion and crystallite size of supported Pd particles. These ratios are respectively 0.08, 0.04, and 0.44 for Pd(WO_3calc), Pd/(WO_3red), and Pd/(WO_2red) before reduction. The Pd/W atomic ratio deduced from microanalysis taking into account the nature of the support (WO_3, WO_2) is approximately 0.052. This value is in the scale of size of that found for Pd–WO_3-based catalysts which is correlated to a good dispersion, which can then explain the high activity. The higher activity observed for Pd/(WO_3calc) could be attributed to a higher density of accessible metallic sites. Pd/(WO_2red) catalyst will be initially less active corresponding to the poor dispersion of metal and probably to a higher crystallite size (35).

From the 2MP and 4M1Pn reactants, the catalysts give predominantly isomerization (80–90%) with a 3MP/HEX ratio higher than 1 and the formation of 23DB which supposes the presence of acidic sites. As expected for acidic catalysts, β-scission is the major reaction for the cracking leading to propane. The product distributions are clearly different from those obtained with Pd/Al_2O_3, well known for its cyclic mechanism for isomerization and its selective terminal demethylation (15, 17, 48, 49). The contribution of palladium could be directly associated with the presence of MCP (intermediate of reaction) and C1 + C5 products. This is not clearly the case, even if small quantities of MCP are initially detected. Moreover, the selectivity in isomers for Pd/Al_2O_3 never exceeds 10% (Table 2). At this stage, by comparison with bulk tungsten oxide properties (WO_3 and WO_2) and in agreement with other studies on metal–tungsten-based catalysts, we attribute these acidic properties to some tungsten oxides phases only (10, 11, 37). The chlorine initially detected on as-prepared catalysts could not be responsible for acidity character. Indeed, we showed previously by XPS experiments that chlorine was no longer detected at the surface after the catalysts were reduced (35). The differences observed in the 3MP/HEX values between the catalysts clearly demonstrate a difference in the acidic strength, which is closely related to the nature of the tungsten oxide phases formed at the surface. Physical and chemical characterizations of the catalysts revealed that before any reduction, the surfaces are composed of WO_3 crystalline phase for Pd–WO_3-based catalyst and WO_3 with WO_2 for Pd(WO_2red) catalyst (35). The WO_3 phase obtained for Pd(WO_2red) results from contamination of WO_2 due to oxidation during air exposure. The initial isomerization properties ($t = 0.25$ h under H_2 at 350°C) could not be directly attributed to the presence of WO_3 phase. Indeed, after a short induction time under H_2 at 350°C, no drastic changes are observed. Pd/(WO_3calc) and Pd(WO_3red) exhibit identical properties which is linked to a stabilization of their surface states. In agreement with XPS and XRD results (35), we attribute the stability of properties to the formation of the well-defined nonstoichiometric $W_{20}O_{58}$ phase. The reduction of WO_3 in $W_{20}O_{58}$ occurs rapidly in a homogeneous process at the surface as well as in the bulk for Pd–WO_3-based catalysts, in agreement with previous studies (42, 50–52). $W_{20}O_{58}$ oxide is known to be a stable nonstoichiometric phase. This is consistent with a computer simulation related to the reduction of modeled WO_3 surfaces (53). According to these observations, shorter induction times should be necessary to observe more drastic changes in the product distributions. In the case of Pd(WO_2red) catalyst, the surface evolution occurs slowly, as demonstrated by XPS measurements (35), and probably results at 350°C, under our operating conditions, from the difficulty in reducing the WO_2 phase which composes the bulk. On this basis, it seems reasonable to consider Pd/(WO_2red) as a catalyst composed of a mixed oxide support such as "Pd/(WO_3–WO_2red)." The WO_3 phase, present as a contaminant in WO_2, exhibits a strong acidic character which is increased, in our opinion, by an interaction with WO_2 in the bulk leading to the high and characteristic 3MP/HEX ratios (initially 8–10). The decrease of the ratio as a function of time under H_2 is significant in the slow appearance of $W_{20}O_{58}$ at the surface, leading to a "Pd/($W_{20}O_{58}$–WO_2)" catalyst. All these factors suggest that the acidic character resulting from the $W_{20}O_{58}$ phase containing both W^{6+} and W^{5+} cations (localized in the shared planes) would be weaker than for the WO_3 phase containing only W^{6+} cations. For each catalyst, the stability of the catalytic properties would be reached as soon as the surfaces become mainly composed by $W_{20}O_{58}$ which is accompanied by some W metal traces (detected by XPS). Our results do not confirm recent reports claiming that the WO_2 phase only possesses dehydrogenation and isomerization properties (12, 13). However, Cornet and Travert had previously attributed the strong acidic character for isomerization toward olefins to the $W_{20}O_{58}$ phase formed by reduction of WO_3 at 400°C (37). The results reported by Ogata *et al.* (10, 54) for hydrocracking of *n*-heptane showed that the reaction products were strongly dependent on the oxidation state of tungsten which determines the reaction mechanism and shows that $WO_{2.87}$ (i.e. $W_{20}O_{58}$) has properties similar to those of "pseudo-WO_2" ($WO_{2-\alpha}$, α small). From the foregoing considerations, it is clear that Pd–W-based catalysts present a complex catalytic behavior. We attributed the acidic character for isomerization developed by such catalysts to tungsten oxidic phases (WO_3, $W_{20}O_{58}$). The stability of the catalysts is reached as soon as the surface is mainly composed of $W_{20}O_{58}$ entities. No further reduction to W^0 is observed as for bulk tungsten oxides (11–13, 39). This suggests that palladium stabilizes and controls in some way the reduction of the support as previously observed for Pt/WO_3/ZrO_2 (55). The acidic character is also confirmed by catalytic results obtained from HEXn leading to 70–90% isomerization as opposed to what was observed for a classical Pd/Al_2O_3 catalyst giving only ~8% of isomers and a nonnegligible percentage of MCP (results not presented). This is also consistent with ring enlargement predominance for the MCPn reactant which required acidic sites (56) whereas hydrogenolysis is the major reaction observed for classical metallic palladium catalyst. MCPn and MCP seem to be good probe molecules to determine the presence of metallic or acidic functions. The decreasing order in hydrocarbon reactivity confirms that the reaction is mainly controlled by acidic properties of the surface: $4M1Pn \gg 2MP > HEXn \ggg MCPn$ on Pd–W-based catalysts and $MCP \gg 2MP$, $4M1Pn \ggg HEX$ on Pd/Al_2O_3.

If the properties of supports which induced skeletal isomerization are clear, what is then really the role of palladium in such catalytic systems? Although the distribution of products does not give the fingerprint of palladium, some observations could ensure its participation. We found that palladium allows initially the conversion of saturated hydrocarbon (2MP) and shows its intrinsic catalytic properties, identified by MCP traces in product distributions. Palladium can initially be required for C–H dissociation leading to the olefin precursor. Indeed, the difference between the 2MP and 4M1Pn reactivities shows that dehydrogenation is the limiting step which suggests that initially catalysts are bifunctional. A metallic function is required at the initial step of alkane conversion but also for rehydrogenation before the desorption step. Nevertheless, how can we explain that palladium present at the surface and in its metallic form even before any treatment (35) cannot ensure isomerization via a typical metallic mechanism? One explanation may be the existence of a geometric metal–support interaction as suggested by Zhang *et al.* to explain the activity decrease in the $CO + H_2$ reaction when palladium is supported on WO_3 rather than Al_2O_3 (23). The authors did not exclude incorporation of metal in the framework of the support and specified that the synergy between Pd and W would be more important than the Pd particle size effect for catalyst activity. The existence of a Pd–WO_x interface ("WO_x patches decorating Pd particles") was also suggested by L'Argentière Figoli (25) to explain the better activity and the thio resistance of Pd/WO_3 catalyst for selective hydrogenation. To explain the values of the Pt/W atomic ratio and the catalytic results in re-forming obtained on Pt–W/Al_2O_3 reduced under H_2 at 400°C, M'Boungou *et al.* concluded that an interaction between Pt and the support led to a migration of WO_x entities onto Pt particles (29, 30). The same proposal was put forth for Pt/WC_x–Al_2O_3 and Pd/WO_3 systems to explain the inhibition of the catalytic performance (27, 28). We have no argument to propose such a geometrical SMSI phenomenon. Indeed, the Pd/W ratio deduced from *in situ* XPS experiments does not allow us to imagine a coverage of Pd particles by WO_x entities (35). Anchoring of metal particles by WO_x entities would imply an increase of the Pd/W atomic ratios in XPS. Moreover, a geometric interpretation is not in agreement with catalytic results obtained after a short time under H_2 at 350°C for Pd–WO_3-based catalysts and after a longer time for Pd/(WO_2red). Indeed, we have suspected the palladium participation and clearly demonstrated that the disappearance of the metallic properties was recovered by oxidation under air at 400°C. Even

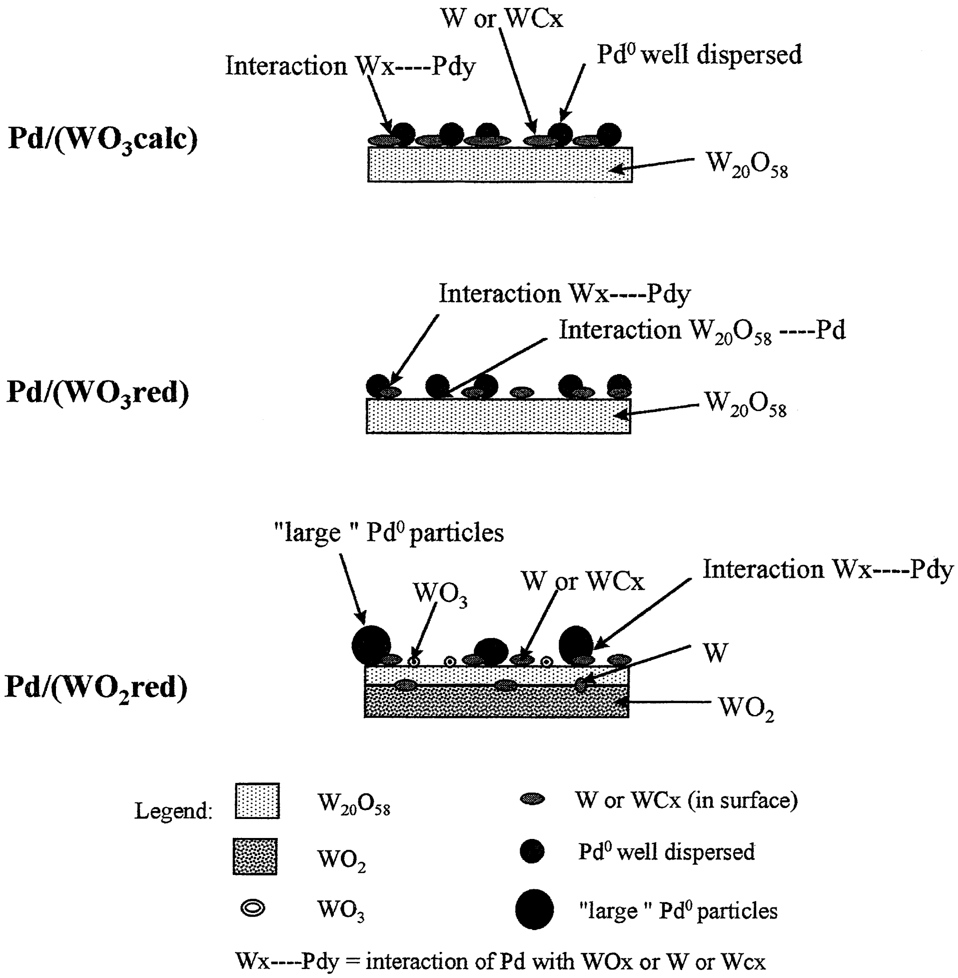

FIG. 7. Schematic representation of surface states for stabilized catalysts under H_2 at 350°C.

if such a phenomenon is generally observed in the case of geometrical SMSI, we consider that the low temperature of reduction (350°C) compared to previous results does not allow the creation of mobile WO_x entities. However, we point out that the disappearance of Pd catalytic properties not only depends on time under H_2, but may also partly result from deactivation due to the successive catalytic tests. That is why we suggest an electronic effect between Pd and W species to explain the change in the Pd properties as previously proposed (57, 58). Contreras and Fuentes found that addition of W to Pt/Al_2O_3 catalysts stabilizes and increases the dispersion after high-temperature reduction which was attributed to the formation of Pt species bound to WO_x during drying and calcination and to strong interaction between Pt crystallites and mixed oxide after reduction (59). To explain why palladium does not act as expected for the C–H cleavage, we propose the appearance of an electronic interaction between Pd and tungsten species ($Pd_x \leftrightarrow W_y$) under H_2, although we have not recorded changes in the Pd binding energy by XPS. The dilution or dispersion of Pd, W, or WC_x sites would allow H_2 dissociation and partial olefins rehydrogenation but not the simple or multiple hydrogenolysis which requires larger sites for multiple adsorptions (60). From this point of view, we can conclude that $Pd/(WO_2red)$, the less active but much longer active catalyst toward saturated hydrocarbon, is less dispersed and contains relatively large particles. The difference in activities between the three catalysts would result not only from Pd dispersion but also from the metallic W^0 sites present at the surface. We present in Fig. 7 a schematic model for the three $Pd/(WO_x)$ catalysts after stabilization, based on our catalytic results and experimental characterizations (35).

Catalysts submitted to HTR treatments. Reduction at 600°C leads to very active and selective catalysts for isomerization of 2MP and 4M1Pn regardless of the time under H_2. As for LTR treatments, $Pd–WO_3$-based catalysts are slightly more active than $Pd/(WO_2red)$ catalyst. After 5 h under H_2, a steady state is observed showing a real stability in isomerization (85–90%). No deactivation occurs regardless of the time under H_2. Product distributions reflect here again an acidic character for isomerization, which is verified by the products formed with other hydrocarbons such as HEX, MCP, and 22DB. As pointed out by Burch and Paal (61), 22DB can be use as a probe molecule to characterize metal catalysts. In most of the cases, the major reaction of 22DB over a metal is hydrogenolysis. The isomerization reaction never exceeds 70% and is linked to the influence of some parameters, such as high temperature of reduction, H_2 pressure, and carbonaceous deposit, which are involved in the modification of the crystallite sizes or the break-up of the large ensembles of metal atoms. So, generally, the increase in the reaction of isomerization is accompanied by a decrease in activity which is not observed in our case. The patterns of hydrogenolyzed and isomerized (mainly 23DB) products show that Pd is not involved in these reactions and confirm an acidic function participation. In addition to what was observed for LTR treatments, the difference in activities between 2MP and 4M1Pn is not so characteristic and similar rate values are obtained. By XPS and XRD techniques, we clearly demonstrated the existence of Pd^0 and W^0 plus W^{5+} and W^{6+} (35). But there is no evidence for W^0 or WC_x properties well known to give extensive hydrogenolysis (11, 28, 60, 62, 63). Pd contribution in skeletal rearrangement cannot be totally excluded. MCP and $C1+C5$ products are observed in higher quantities than those observed for LTR treatments. On the other hand, in contrast to what was observed for bulk WO_3 powder treated under H_2 at a temperature higher than 550°C showing changes in the product distribution, we suggest the stabilization of tungsten entities at the surface by Pd (interaction, alloy or bimetallic phase) allowing hydro–dehydrogenation associated with an active acidic phase such as $W_{20}O_{58}$ for high isomerization selectivity. However, it is difficult to imagine that the $W_{20}O_{58}$ phase could resist at 600°C under H_2, when it is normally destroyed at 420°C. So another highly reduced phase has to be considered. Whittingham and Dickens showed that WO_3 was easily converted to metallic tungsten (α-W or β-W) under H_2 between 500–600°C (64). So we argue, as mentioned in Part I of this article (35), that the reduction of the $W_{20}O_{58}$ phase to α-W occurred via the β-W phase (i.e., W_3O) as mentioned by Schubert (42), is stable under our operating conditions. This phase should be responsible for (de)hydrogenation and isomerization reactions, acting in that way as a monofunctional catalyst. The initial evolutions observed in the products indicate a modification in the surface states of catalysts correlated to structural modifications. In the case of Pd-WO_3-based catalysts, these evolutions can be illustrated by the distribution of cracked products and the 3MP/HEX ratio. The cracking leads initially to selective demethylation ($C1+C5$) and β-scission (C3) and then mainly to $C1+C5$ for stable surfaces. At the same time the 3MP/HEX ratio goes from 1 to 3.5. These changes are induced by the surface state modifications as was observed for LTR treatments (rapid transformation $WO_3 \rightarrow W_{20}O_{58}$) leading to the increase of the reduction process with the formation of the metastable W_3O phase. In the case of the Pd/(WO_2red) catalyst, cracked products initially formed are $C1+C5$. After 5 h under H_2 at 600°C, mainly C3 is formed and then $C1+C5$ are the major cracked products. The 3MP/HEX ratio rapidly decreases from 20 ($t=25$ h) to 3.5 ($t=0.20$ h) via 1.5 ($1<t<15$ h) values. These modifications are linked to the reduction process of the WO_2 support (i.e., "WO_3/WO_2") as follows: $WO_3 \rightarrow W_{20}O_{58}$ (slowly) $\rightarrow W_3O$. The disappearance of the acidic function is deduced from the decrease of the C3 formation (Pd–WO_3-based catalysts) and from the decrease of the 3MP/HEX ratio (Pd/(WO_2red catalyst)). As for the LTR catalysts, we think that palladium associated with the highly reduced tungsten oxide phase (W_3O) could allow rehydrogenation and dehydrogenation (C–H cleavage) that is necessary to observe the 2MP activity. Schematic models of stabilized surfaces are illustrated in Fig. 8.

4.2. *Deactivation Phenomena*

We already pointed out the extremely rapid decrease of Pd(WO_3calc) and Pd(WO_3red) activity toward alkanes at 350°C under H_2 during successive and alternative catalytic tests with 2MP and 4M1Pn, indicating a deactivation of the metallic function necessary for hydro–dehydrogenation reactions, probably due to hydrocarbon residue deposits. Indeed, the results obtained after 15 h under H_2 at 350°C without intermediate pulses of HC revealed an activity for the catalysts toward the alkane (2MP) whereas during the same time of exposure under H_2 but with successive pulses of hydrocarbons, a total inactivity was observed. The deactivation is slower for Pd/(WO_2red). We have attributed the metallic character to the palladium in the interaction with W species (Pd–WC_x or $W_{20}O_{58}$) and the difference in activity observed between the catalysts to the dispersion of the metallic phase. These proposals seemed to be confirmed by the deactivation phenomena. Indeed, we have assumed that the dispersion of the metallic sites for Pd–WO_3-based catalysts will be higher than for Pd/(WO_2red) catalyst. Consequently, at the same palladium loading, the metallic particle size will be higher for Pd/(WO_2red) catalyst. Smaller crystallites are more sensitive to hydrocarbon poisoning. A higher density of metallic sites, as for Pd/WO_3-based catalysts, will induce a higher activity leading to a rapid self-poisoning of metallic sites by carbonaceous residue. This suggestion is in accordance with the results of Contreras and Fuentes (59), showing that reduction at 800°C produced Pt/WO_3–Al_2O_3 catalysts with lower initial activity toward benzene hydrogenation and with higher deactivation resistance, but seems to contradict previous results obtained for the Pt/WO_3/ZrO_2 system (63). The deactivation phenomenon is selective to metallic sites and the catalysts remain active toward olefins. The

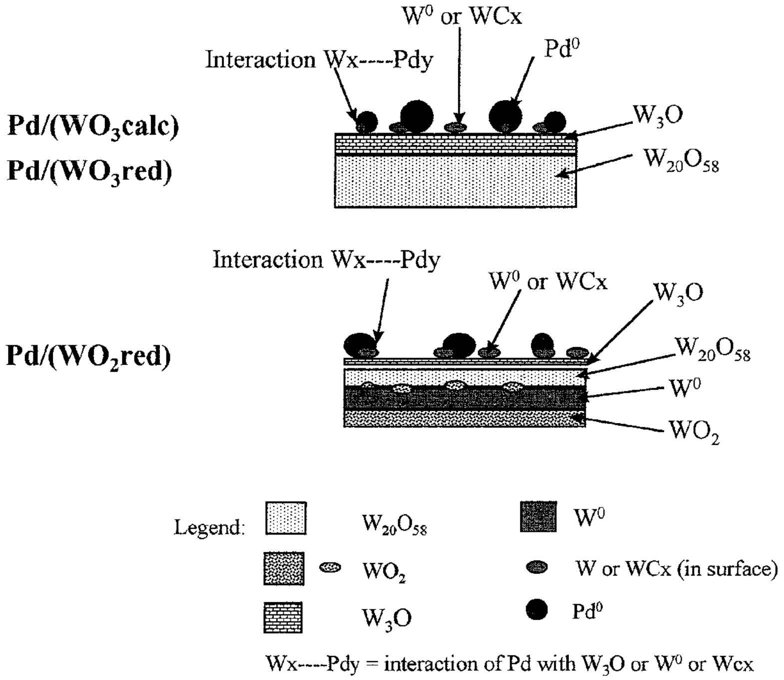

FIG. 8. Schematic representation of surface states for stabilized catalysts under H_2 at 600°C.

acidic function is not affected in the same way and is not as sensitive to hydrocarbons which was confirmed by experiments achieved under continuous 4M1Pn/H_2 mixture (Section 3.1.3). No deactivation occurred and only slight evolution of the product distribution was observed (C3 decreases and S_{iso} increases) which is not the case for metal-free catalyst like WO_x/Al_2O_3. Indeed, Benitez *et al.* studied the catalytic behavior of WO_x/Al_2O_3 catalysts for skeletal isomerization of 1-butene (66) and observed a coke deposit during the reaction. In the same way, Ponec *et al.* (8) demonstrated that a high density of actives sites causes severe WO_3/Al_2O_3 deactivation for skeletal isomerization of 1-butene due to catalyst carbonization induced by polymerization of activated isobutene. At a low density of active sites, the isobutene molecules are so far from each other that no polymerization occurs. The catalytic results obtained on Pd–tungsten-based catalysts treated under H_2 at 350°C for a short time have been interpreted by the way of a bifunctionality which required the participation of both metallic and acidic sites. According to Sachtler's results (56) on ring enlargement over bifunctional catalysts (Pt/HY), we think that the metallic sites protect the acidic sites against deactivation by deposition of a carbonaceous residue but that coke precursors formed on acidic sites contribute to deactivate palladium which can no longer maintain its intrinsic properties and then is only able to dissociate H_2 and partly (de)hydrogenates. However, the higher the Pd dispersion, the higher is the density of actives sites and consequently the higher is the reactivity, leading to a rapid deposition of carbonaceous residue covering partially or quasi totally the metal particles. The distance between acidic and metallic sites influencing H transfers is also an important factor for deactivation. As mentioned previously (67, 68), the metal in the vicinity of acid sites, which is required for H_2 dissociation and then hydride transfers, is an important parameter for bifunctional catalysts. Manoli *et al.* (68) named these centers of acid–metal co-operation "compressed bifunctional sites." Interesting implications were given by results obtained after pure H_2 exposures at 350°C. In neither case did H_2 exposures lead to the modifications in activity excepted for 4M1Pn on Pd/(WO_2red) catalyst for which a great enhancement of the activity was observed. In that case, the distance between acidic and metallic sites would be such that only a part of the acidic sites would be sufficiently close to metal particles to avoid deactivation. Furthermore, we also must underline the modification of the selectivity in isomers, which is lower just after H_2 exposure for most of the cases, and the details of cracked products show a preference for β-scission reaction. This can be attributed to competition between isomerization and hydrogenolysis reactions, probably resulting from the carbocation desorption step which strongly depends on the H_2 concentration. Although pure H_2 is not able to regenerate the 2MP reactivity on Pd–WO_3-based catalysts, we found that just after an oxidative treatment under air at 400°C, catalysts retrieve their activity for 2MP. We noted also an increase in CH_4 among the product distribution just after the oxidation which led us to confirm that metal activity is linked to the existence of WC_x species. This is also confirmed by the increase of cracked products, mainly methane (Fig. 6), just after $[O_2 + H_2O + N_2]$ exposures applied in the case of the Pd/(WO_2red) catalyst.

4.3. *Nature of Acidic Sites*

Pd–W-based catalysts reduced at 350°C show interesting selectivity in isomerization which is correlated to acidic properties, closely related to the tungsten oxide phase formed at the surface upon reduction. In the literature, the existence of Brønsted and Lewis sites on tungsten oxides is well accepted. However, the localization and the nature of Lewis sites are not well-defined and the genesis of Brønsted sites is not clear. Cornet and Travert associated Lewis acid sites generated under reduction of WO_3 with W^{5+} species localized in the shared planes of $W_{20}O_{58}$ phases (37), whereas Kamiya and Ogata concluded that the Lewis acidic character is caused by an anion vacancy (54). FTIR investigations on WO_3 material indicated two types of strong Lewis acidic sites as well as Brønsted acidic sites (69). The authors suggested that coordinately unsaturated W^{6+} ions, located at the pseudocubic faces of WO_3, would act as strong Lewis acidic sites, according to the high charge, the small ionic radii, and the high electronegativity. We cannot discard the possibility that the acidic character observed on Pd–W-based catalysts is due to acidic Lewis sites. We clearly showed that the WO_3 oxide support was rapidly converted to the $W_{20}O_{58}$ phase whereas the WO_2 support was more difficult to reduce and that WO_3 remains longer at the surface exhibiting a stronger acidic character. According to previous results (69, 70), charges and ionic radii of W could play a role in determining the strength of Lewis acidity. It seems reasonable to consider that the Lewis acidity developed by WO_3 containing W^{6+} cations would be higher than for the $W_{20}O_{58}$ phase containing both W^{6+} and W^{5+} cations. However, the generation of Brønsted acidic sites on Pd–W-based catalysts is more suitable. Various factors are invoked to explain their generation and some authors have agreed to suppose that they are generated under H_2. It has been claimed that H_2 generated and maintained Brønsted acidic sites which are required for *o*-xylene isomerization on Pt/WO_x–ZrO_2 (71). The acidic properties would be related to the ability of WO_x to form $W^{6-n}O_x$-(n-H^+) centers and consequently to its reduction ability. The generation of Brønsted acidic sites was also reported during H_2 treatment on Pt/SO_x–ZrO_2 and a conversion of Lewis sites to Brønsted sites was suggested (72). Dehydration of 2-propanol was investigated over MoO_3 treated with H_2 (73). The increase in activity after reduction at 350°C was assigned to hydrated phase MoO_xH_y or $MoO_{2.5}(OH)$. In contrast, Suarez *et al.* observed that MoO_3/Al_2O_3 does not lead to significant generation of Brønsted sites and that the small amount initially present are completely removed upon reduction (74). Segawa and Hall (75) found that Brønsted acidity could be totally suppressed on supported MoO_3 with extended reduction time. In contrast, Ponec *et al.* (8) reported that reduction by H_2 led to the formation of Brønsted sites on supported WO_3 but led to tungsten bronzes for bulk WO_3. From these works, it is clear that both temperature and time under H_2 are important parameters that control the acidity which, in our opinion, is related to the nature and the reducibility of the oxidic phases. Generation of Brønsted acidic sites under H_2 is inconsistent with our results which seem to prove that Brønsted sites are (re)generated under oxidative treatment as reported elsewhere (8, 76, 70). We have clearly demonstrated that H_2 exposures did not cause significant modifications in activity and selectivity. Conversely, oxidation under air at 400°C led to a significant increase in activity which could be attributed to the increase in the density of acidic sites. We noted also an increase of the acidity strength in the case of Pd/(WO_2red) catalysts (increase of the 3MP/HEX ratio) which can be linked to the large reoxidation of the surface in WO_3 which becomes therefore less reducible due to the interaction $WO_{3(\text{surface})}$–$WO_{2(\text{bulk})}$ (35). The increase in activity and acidity obtained after $[O_2 + H_2O + N_2]$ exposures on Pd/(WO_2red) catalyst provide evidence to ascribe acidity to Brønsted sites. It is worth mentioning that the phenomenon is emphasized after a few exposures. The effect of $[O_2 + H_2O + N_2]$ mixture makes it possible to generate Brønsted sites and to reoxidize the surface (increasing the acidity strength). Adding water to the catalytic feed (H_2/H_2O) was previously reported to increase Brønsted acidic sites, increasing even isomerization (7, 8, 66, 77) or cracking (9, 78). As proposed by Ramis *et al.* (69), we suggest that adsorption of water can lead to hydroxyl groups by a dissociative mechanism. The acidity strength could be rationalized on the basis of the number of terminal oxygen atoms and charge delocalization on W atoms (70, 79). The removal of the protons leads to a negative charge which can be delocalized over the other terminal oxygen atoms. Increasing the delocalization will stabilize the conjugated base, leading to a stronger conjugated acid. A strong interaction between W^{6+} species (WO_3) and "WO_2 support" will induce a higher electron delocalization of terminal oxygen atom to W^{6+} species, considered as charge acceptors, increasing the lability of the proton and so its acidic character. It is likely that the acidity strength is related to the distance between W and O atoms in the structure and thus to the ionicity character of the W^{x+}–OH bond (W^{6+}–OH bond $>W^{5+}$–OH bond). The compactness of the structure can also be invoked. An increase in acidity on WO_3/Al_2O_3 was reported to be due to a crowding of WO_4 groups during a change of configuration from edge-shared to corner-shared tetrahedron (70). It cannot be excluded that polyhedron chaining in the structure induces some modifications in acidity. Indeed, whatever the structure WO_3 and $W_{20}O_{58}$, atoms are octahedrally coordinated but linked from corners and from corners and edges, respectively, and the density of sites is certainly modified.

In conclusion, we propose that Brønsted sites are initially present, produced by the structural surface water. During reduction, the Brønsted site population is maintained resulting from the reduction of support leading to water formation which is adsorbed by W^{x+} cations. Oxygen and water exposures are able to generate Brønsted acidic sites and to increase the strength of acidity (reoxidation of surfaces). The difference in acidity strength could be illustrated as follows (Fig. 9).

4.4. *Mechanistic Approach*

LTR catalysts. Catalysts initially treated under H_2 at 350°C show a higher reactivity toward 4M1Pn than for 2MP which could be explained by the dehydrogenation step (cleavage of C–H) This indicates that metallic sites are required for H_2 dissociation and partly for (re)hydrogenation. Isomerized and cracked products are typical of acidic properties leading mainly to branched hydrocarbons and propane. It seems obvious that the mechanism is initially bifunctional which is confirmed by energies of activation (80), determined in the range 300–350°C for 2MP, giving respectively 18.8 kcal/mol and 14.7 kcal/mol for Pd/(WO_3red) and Pd/(WO_2red). We suggest that isomerization and cracking reactions proceed via a classical "carbocation intermediate" (36). We have not enough information to define more accurately the nature of the intermediate species precursor of the carbocation (carbenium or carbonium species) probably depending on the acid strength of the catalysts. The slight difference in isomerization observed between catalysts having similar tungsten surface composition could result from the interaction of the carbocation with the surface. An alkoxy intermediate species (A in Fig. 10) (36, 78), requiring Brønsted sites, could well illustrate this difference. The small percentage of cracking is explained by H_2 transfer. Indeed, a short H_2 transfer step induces desorption of carbocations before β-scission. H_2 concentration and H_2 storage determine the steady-state carbocation lifetime. A rapid neutralization of carbocation is required to lead a rapid desorption and prevent cracking reaction. Metallic function (Pd_x–W_y) must be mainly involved in these transfers.

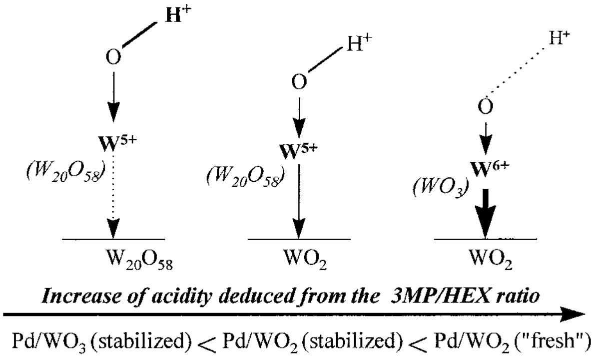

FIG. 9. Schematic representation of Brønsted acidity for Pd–W-based catalysts reduced at 350°C.

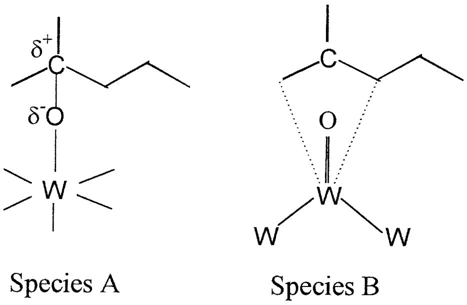

FIG. 10. Schematic of the species involved in a bifunctional metal–acid mechanism (species A) and a monofunctional metal mechanism (species B).

HTR catalysts. 2MP and 4M1Pn hydrocarbons show similar reactivity on stabilized catalysts which is characteristic of a monofunctional mechanism. The demethylation is selective (C1 + C5) and the selectivity in isomers is relatively high. We conclude that the same sites are responsible for cracking and isomerization properties attributed to the metallic W_3O phase. This phase, possessing a metallic character, would be also responsible for (de)hydrogenation properties. A metallacycle mechanism involving tungstenacyclobutane species (Fig. 10) is proposed as established for neopentane isomerization on oxygen-modified WC (36, 60, 63). Pd in association with W could take part in the dehydrogenation of alkane, explaining in that way the small difference between 2MP and 4M1Pn reaction rate. We cannot rule out a Pd contribution in selective demethylation and isomerization via cyclic mechanism. Palladium also gives isomerization via a metallacycle mechanism, leading to bond shift and selective demethylation, which does not require the same intermediate as the species B in Fig. 10.

5. CONCLUSION

The aim of this work was to study Pd/WO_3 and Pd/WO_2 catalytic properties for re-forming of hydrocarbons as a function of various activation treatments. Reduction at 350°C led to stable catalysts due to the formation of the $W_{20}O_{58}$ phase. These phase is obtained as well on the surface as in the bulk for Pd/WO_3 catalysts and only on the surface for Pd/WO_2 catalyst. Catalysts are active for skeletal rearrangements of hexanes and hexenes and very selective toward isomerization. The selectivity in isomerization was correlated to the acidity of oxidic supports developing Brønsted sites. A difference in acidity strength was observed initially under H_2 between Pd/WO_3 and Pd/WO_2.

This difference was correlated to the slowest reduction of WO$_3$ to W$_{20}$O$_{58}$ when WO$_3$ is present as a contaminant of WO$_2$ surfaces (as in the case of Pd/WO$_2$). Consequently, we proposed that the acidic character of WO$_3$ (containing W^{6+}) is higher than for W$_{20}$O$_{58}$ (containing both W^{6+} and W^{5+}). We noted a deactivation of the metallic function, which occurred faster for Pd/WO$_3$ catalysts, leading to a decrease in the reactivity of saturated hydrocarbons. An explanation of these results was based on the speculation of a bifunctional catalyst constituted of a metallic function (Pd$_y$–W$_x$) for hydrodehydrogenation and an acidic function (OH groups) for isomerization involving a carbocation mechanism including alkoxy intermediate species. The presence of oxygen was found to be effective in increasing the catalyst activity and regenerating the metallic function. The effect of H$_2$O traces, exclusively studied for Pd/WO$_2$ catalyst, led to a great increase in the number of acidic sites and in the strength of the acidity. A correlation between the acidic strength and the nature of the oxide has been made. A great improvement in catalyst activity was obtained at a higher reduction temperature (600°C) due to the formation of metallic W. An interesting result was the high and stable selectivity in isomers that we attributed to the W$_3$O phase. In this case we proposed a metallacycle mechanism involving tungstenacyclobutane species. We do not rule out the possibility that Pd participates in the (de)hydrogenation reaction. In neither case does Pd exhibit its intrinsic catalytic properties which is explained by an electronic interaction Pd $\leftrightarrow$ W. No catalyst deactivation was observed in that case.

REFERENCES

1. Grunert, W., Shpiro, E. S., Feldhaus, R., Anders, K., Antoshin, G. V., and Minachev, K. M., *J. Catal.* **107**, 522 (1987).
2. Kazuta, M., and Tanaka, K. I., *J. Catal.* **123**, 164 (1990).
3. Rodriguez-Ramos, I., Guerrero-Ruiz, A., Homs, N., Ramirez de la Piscina, P., and Fierro, J. L. G., *J. Mol. Catal. A: Chemical* **95**, 147 (1995).
4. Van Roosmalen, A. J., and Mol, J. C., *J. Catal.* **78**, 17 (1982).
5. Haber, J., Janas, J., Schiavello, M., and Tilley, R. J. D., *J. Catal.* **82**, 395 (1983).
6. Yamaguchi, T., Tanaka, Y., and Tanabe, K., *J. Catal.* **65**, 442 (1980).
7. Baker, B. G., and Clark, N. J., *in* "Catalysis and Automotive Pollution Control" (A. Crucq and A. Frennet, Eds.), Stud. Surf. Sci. Catal. 30, p. 483. Elsevier, Amsterdam, 1987.
8. Gielgens, L. H., Van Kampen, M. G. H., Broek, M. M., Van Hardeveld, R., and Ponec, V., *J. Catal.* **154**, 201 (1995).
9. Xing Cheng, Z., and Ponec, V., *Catal. Lett.* **25**, 337 (1994).
10. Ogata, E., Kamiya, Y., and Ohta, N., *J. Catal.* **29**, 296 (1973).
11. Katrib, A., Hemming, F., Wehrer, P., Hilaire, L., and Maire, G., *J. Electron. Spectrosc. Relat. Phenom.* **76**, 195 (1995).
12. Katrib, A., Logie, V., Saurel, N., Wehrer, P., Hilaire, L., and Maire, G., *Surf. Sci.* **377**, 754 (1997).
13. Katrib, A., Logie, V., Peter, M., Wehrer, P., Hilaire, L., and Maire, G., *J. Chim. Phys.* **94**, 1923 (1997).
14. Karpinski, Z., *Adv. Catal.* **37**, 45 (1990).
15. Hajek, M., Corolleur, S., Corolleur, C., Maire, G., O'Cinneide, A., and Gault, F., *J. Chim. Phys.* **71**, 1229 (1974).
16. Finlayson, O. E., Clarke, J. K. A., and Rooney, J. J., *J. Chem. Soc., Faraday Trans. 1* **80**, 191 (1984).
17. Le Normand, F., Kili, K., and Schmitt, J. L., *J. Catal.* **139**, 234 (1993).
18. Paal, Z., and Tetenyi, P., *Appl. Catal.* **1**, 9 (1981).
19. Lomot, D., Juszczyk, W., and Karpinski, Z., *Appl. Catal. A: General* **155**, 99 (1997).
20. Ivanova, I. I., Seirvert, M., Pasau-Claerbout, A., Blom, N., and Derouane, E. G., *J. Catal.* **164**, 347 (1996).
21. Juan, A., Moro, C. C., and Damiani, D. E., *Colloids Surf. A* **122**, 257 (1997).
22. Yermakov, Yu. I., Kuznetsov, B. N., and Ryndin, Yu. A., *J. Catal.* **42**, 73 (1976).
23. Zhang, R., Schwartz, J. A., Datye, A., and Baltrus, J. P., *J. Catal.* **138**, 55 (1992).
24. Regalbuto, J. R., Fleisch, T. H., and Wolf, E. E., *J. Catal.* **107**, 114 (1987).
25. L'Argentière, P. C., and Figoli, N. S., *Catal. Lett.* **53**, 149 (1998).
26. Adams, K. M., and Gandhi, H. S., *Ind. Eng. Chem. Prod. Res. Dev.* **22**, 207 (1983).
27. Jackson, S. D., Brandreth, B. J., and Winstanlay, D., *Appl. Catal.* **27**, 325 (1986).
28. Katrib, A., Hemming, F., Wehrer, P., Hilaire, L., and Maire, G., *Topics Catal.* **1**, 75 (1994).
29. M'Boungou, J. S., Schmitt, J. L., Maire, G., and Garin, F., *Catal. Lett.* **10**, 391 (1991).
30. M'Boungou, J. S., Hilaire, L., Maire, G., and Garin, F., *Catal. Lett.* **10**, 204 (1991).
31. Farbokto, J. M., Garin, F., Girard, P., and Maire, G., *J. Catal.* **139**, 256 (1993).
32. Kuznetsov, B. N., Yermakov, Yu. I., Boudart, M., and Collman, J. P., *J. Mol. Catal.* **4**, 49 (1978).
33. Vaudagna, S. R., Carravese, S. A., Comelli, R. A., and Figoli, N. S., *Appl. Catal. A: General* **168**, 93 (1998).
34. Hino, M., and Arata, K., *Appl. Catal. A: General* **169**, 151 (1998).
35. Bigey, C., Hilaire, L., and Maire, G., *J. Catal.* **184**, 406 (1999).
36. Garin, F., Keller, V., Ducros, R., Muller, A., and Maire, G., *J. Catal.* **166**, 136 (1997).
37. Cornet, D., and Travert, G., Final Report DGRST, Paris, 1975.
38. Logie, V., Wehrer, P., Katrib, A., and Maire, G., *J. Catal.* **189**, 438 (2000).
39. Bigey, C., Logie, V., Bensaddik, A., Schmitt, J. L., and Maire, G., *in* "Rayon X et Matière, Proceedings" (A. Cornet and N. Broll, Eds.), J. Phys. IV. 815, p. 553. EDI Sciences, Strasboury, 1998.
40. Sahle, W., and Berglung, S., *J. Less-Common Metals* **79**, 271 (1981).
41. Arnoldy, P., De Jong, J. C. M., and Moulijn, J. A., *J. Phys. Chem.* **89**, 4517 (1985).
42. Schubert, W. D., *J. Ref. Hard Metals* **9**, No. 4, 178 (1990).
43. Sancier, K. M., *J. Catal.* **23**, 298 (1971).
44. Khobiar, S., *J. Phys. Chem.* **68**, 411 (1964).
45. Benson, J. E., Khon, H. W., and Boudart, M., *J. Catal.* **5**, 307 (1966).
46. Larsen, G., Lotero, E., and Parra, R. D., *in* "11th International Congress on Catalysis" (J. W. Hightower, W. N. Delgass, E. Iglesia, and A. T. Bell, Eds.), Stud. Surf. Sci. Catal. 101, p. 543. Elsevier, Amsterdam, 1996.
47. Iglesia, E., Barton, D. G., Soled, S. L., Miseo, S., Baumgartner, J. E., Gates, W. E., Fuentes, G. A., and Meitzner, G. D., *in* "11th International Congress on Catalysis" (J. W. Hightower, W. N. Delgass, E. Iglesia, and A. T. Bell, Eds.), Stud. Surf. Sci. Catal. 101, p. 533. Elsevier, Amsterdam, 1996.
48. Paal, Z., and Tetenyi, P., *React. Kinet. Catal. Lett.* **12**, 131 (1975).
49. Muller, J. M., and Gault, F., *J. Catal.* **27**, 361 (1972).
50. Haber, J., Stoch, J., and Ungier, L., *J. Solid State Chem.* **19**, 113 (1976).
51. Biloen, P., and Pott, G. T., *J. Catal.* **30**, 169 (1973).
52. Chappell, P. J. C., Kibel, M. H., and Baker, B. G., *J. Catal.* **110**, 139 (1988).

53. Oliver, P. M., Parker, S. C., Edgell, R. G., and Jones, F. H., *J. Chem. Soc., Faraday Trans.* **96**(12), 2049 (1996).
54. Kamiya, Y., and Ogata, E., *in* "5th International Congress on Catalysis" (J. E. Hightower, Ed.), Catalysis 2, p. 1291. North-Holland, Amsterdam, 1972.
55. Soled, S. L., AIChE Annual Meeting, paper **85**, 1994.
56. Chow, M., Park, S. H., and Sachtler, W. M. H., *Appl. Catal.* **19**, 349 (1985).
57. Yermakov, Yu. I., Kuznetov, B. N., and Ryndin, Yu. A., *J. Catal.* **42**, 73 (1976).
58. Ioffe, M. S., Kuznetsov, B. N., Ryndin, Yu. A., and Yermakov, Yu. I., *Stud. Surf. Sci. Catal.* **131**, (1976).
59. Contreras, J. L., and Fuentes, G. A., *in* "11th International Congress on Catalysis" (J. W. Hightower, W. N. Delgass, E. Iglesia, and A. T. Bell, Eds.), Stud. Surf. Sci. Catal. 101, p. 1195. Elsevier, Amsterdam, 1996.
60. Hemming, F., Wehrer, P., Katrib, A., and Maire, G., *J. Mol. Catal. A: Chem.* **124**, 39 (1997).
61. Burch, R., and Paal, Z., *Appl. Catal. A* **114**, 9 (1994).
62. Muller, J. M., and Gault, F. G., *Bull. Soc. Chim. Fr.* **2**, 416 (1970).
63. Ribeiro, F. H., Dalla Betta, R. A., Boudart, M., Baumgartner, J., and Iglesia, E., *J. Catal.* **130**, 86 (105).
64. Whittingham, M. S., and Dickens, P. G., "Proceedings, 7th Int. Symposium on Reactivity of Solids" (J. S. Anderson, M. W. Roberts, and F. S. Stone, Eds.), Paper 8.6, Chapman et Hall, London, 1972.
65. Larsen, G., Lotero, E., Raghavan, S., Parra, R. D., and Querini, C. A., *Appl. Catal. A* **139**, 201 (1996).
66. Benitez, V. M., Querini, C. A., Figoli, N. S., and Comelli, R. A., *Appl. Catal. A* **178**, 205 (1999).
67. Iglesia, E., Soled, S. L., and Kramer, G. M., *J. Catal.* **144**, 238 (1993).
68. Manoli, J. M., Potvin, C., Mulher, M., Wild, U., Resofszki, G., Buchholz, T., and Pall, Z., *J. Catal.* **178**, 338 (1998).
69. Ramis, G., Cristiani, C., Elmi, A. S., and Villa, P., *J. Mol. Catal.* **61**, 319 (1990).
70. Bernholc, J., Horsley, J. A., Murrell, L. L., Shermann, L. G., and Soled, S., *J. Phys. Chem.* **91**, 1526 (1987).
71. Barton, D. G., Soled, S. L., Fuentes, G. A., and Iglesia, E., *J. Catal.* **181**, 57 (1999).
72. Ebitani, K., Tsuji, J., Hatorri, H., and Kita, K., *J. Catal.* **135**, 609 (1992).
73. Matsuda, T., Hirata, Y., Sakagami, H., and Takahashi, N., *Chem. Lett.* 1261 (1997).
74. Suarez, W., Dumesic, J. A., and Hill, C. G., Jr., *J. Catal.* **94**, 408 (1985).
75. Segawa, K., and Hall, W. K., *J. Catal.* **77**, 221 (1982).
76. Na, K., Okuhra, T., and Misono, M., *J. Catal.* **170**, 96 (1997).
77. Ogata, A., Kazusaka, A., Yamazaki, A., and Enyo, M., *Chem. Lett.* **1**, 15 (1989).
78. McVicker, G. B., Kramer, G. M., and Ziemak, J. J., *J. Catal.* **83**, 286 (1983).
79. Soled, S. L., McVicker, G. B., Murrell, L. L., Shermann, L. G., Dispenziere, N. C., Hsu, S. L., and Waldman, D., *J. Catal.* **111**, 286 (1988).
80. Belloum, M., Travers, Ch., and Bournonville, J. P., *Rev. IFP* **46**, 89 (1991) (Ed. Technip).